Magnetic order and sign of the Dzyaloshinskii–Moriya interaction in 2-D antiferromagnet Ba2CoGe2O7 under applied magnetic field

Henrik Thoma, Vladimir Hutanu, Rajesh Dutta, Arsen Gukasov, Vilmos Kocsis, Yusuke Tokunaga, Yasujiro Taguchi, Yoshinori Tokura, István Kézsmárki, Georg Roth, Manuel Angst

Angaben zur Veröffentlichung / Publication details:

Thoma, Henrik, Vladimir Hutanu, Rajesh Dutta, Arsen Gukasov, Vilmos Kocsis, Yusuke Tokunaga, Yasujiro Taguchi, et al. 2022. "Magnetic order and sign of the Dzyaloshinskii–Moriya interaction in 2-D antiferromagnet Ba2CoGe2O7 under applied magnetic field." *IEEE Transactions on Magnetics* 58 (2): 1–5. https://doi.org/10.1109/tmag.2021.3082983.

Magnetic Order and Sign of the Dzyaloshinskii–Moriya Interaction in 2-D Antiferromagnet $Ba_2CoGe_2O_7$ Under Applied Magnetic Field

Henrik Thoma[1,2], Vladimir Hutanu[1,2], Rajesh Dutta[1,2], Arsen Gukasov[3], Vilmos Kocsis[4,5,6], Yusuke Tokunaga[4,7], Yasujiro Taguchi[4], Yoshinori Tokura[4,8,9], István Kézsmárki[10], Georg Roth[2], and Manuel Angst[11]

[1]Jülich Centre for Neutron Science (JCNS) at Heinz Maier-Leibnitz Zentrum (MLZ), Forschungszentrum Jülich GmbH, 85748 Garching, Germany
[2]Institute of Crystallography, RWTH Aachen University, 52056 Aachen, Germany
[3]Laboratoire Léon Brillouin, CEA-CNRS, CE-Saclay, 91191 Gif-sur-Yvette, France
[4]RIKEN Center for Emergent Matter Science (CEMS), Wako 351-0198, Japan
[5]Department of Physics, Budapest University of Technology and Economics, 1111 Budapest, Hungary
[6]MTA-BME LendŁulet Magneto-Optical Spectroscopy Research Group, Budapest University of Technology and Economics, 1111 Budapest, Hungary
[7]Department of Advanced Materials Science, The University of Tokyo, Kashiwa 277-8561, Japan
[8]Quantum-Phase Electronics Center, Department of Applied Physics, The University of Tokyo, Tokyo 113-8656, Japan
[9]Department of Applied Physics, The University of Tokyo, Tokyo 113-8656, Japan
[10]Experimental Physics 5, Center for Electronic Correlations and Magnetism, Institute of Physics, University of Augsburg, 86159 Augsburg, Germany
[11]Jülich Centre for Neutron Science JCNS and Peter Grünberg Institut PGI, JARA-FIT, Forschungszentrum Jülich GmbH, 52425 Jülich, Germany

The Dzyaloshinskii–Moriya interaction (DMI), i.e., the antisymmetric part of the exchange coupling tensor, favors the perpendicular arrangement of magnetic moment, thus inducing canting in otherwise collinear structures. The DMI is the prerequisite for the emergence of weak ferromagnetism in antiferromagnets, but can stabilize twisted magnetic textures, such as spin spirals, soliton lattices, and magnetic skyrmions. While the magnitude of the DMI determines the canting angle of adjacent spins, its sign dictates the sense of the spin rotation. Based on focused polarized neutron diffraction (PND) study, combined with symmetry analysis, we determine the sign of the DMI in the unconventional multiferroic $Ba_2CoGe_2O_7$ and reveal its detailed magnetic structure in magnetic fields applied in the tetragonal plane. As PND gives unique access to the scattering contribution from the phase-sensitive nuclear-magnetic interference, it is a valuable tool for a straightforward DMI sign determination in bulk materials and allows to disclose even very weak magnetic moments. Remarkably, the sign of the DMI could be determined from the PND measurement of a single reflection, which is demonstrated to be reliable for a large range of applied magnetic field directions and values.

Index Terms— **Dzyaloshinskii–Moriya interaction (DMI), multiferroics, polarized neutron diffraction (PND), weak ferromagnets.**

I. Introduction

THE antiferromagnetic (AFM) $Ba_2CoGe_2O_7$ has aroused great interest in current condensed matter research over the last decade, starting in 2008 when the appearance of ferroelectricity below the magnetic ordering temperature and a strong in-plane anisotropy were first reported [1]. Since the observed unique behavior of the electric polarization with changing magnetic field in $Ba_2CoGe_2O_7$ could not be explained by existing models, Yi *et al.* [1] attributed these effects to the presence of the Dzyaloshinskii–Moriya interaction (DMI) [2], [3]. The antisymmetric DMI is allowed by the noncentrosymmetric space group $P\bar{4}2_1m$ of $Ba_2CoGe_2O_7$. Subsequently, to better explain the unconventional multiferroicity, a novel spin-dependent p-d hybridization mechanism [4] and a spontaneous toroidic effect mechanism [5] were proposed. Spin-nematic interactions were also suggested as origin for the experimentally observed peculiar behavior of the induced polarization [6]. This large variety of new models instigated further detailed studies of $Ba_2CoGe_2O_7$, including a detailed determination of the crystal and magnetic structure in the ground state [7]–[9] and a theoretical symmetry analysis, identifying most of the observed peculiar effects as symmetry-forced results of the weak ferromagnetic (WFM) canting, resulting from the DMI [10]. This further endorses the DMI as a fundamental basis for the emergence and understanding of the unconventional multiferroic behavior observed in $Ba_2CoGe_2O_7$. As the electric polarization changes the sign with increasing magnetic field, not only the magnitude of the DMI exchange constant but also its sign is of particular interest. However, to the best of our knowledge, no study on the DMI aspects in regard to $Ba_2CoGe_2O_7$ has been published yet.

Manuscript received March 16, 2021; revised May 18, 2021; accepted May 18, 2021. Date of publication May 24, 2021; date of current version January 20, 2022. Corresponding authors: H. Thoma and V. Hutanu (e-mail: h.thoma@fz-juelich.de; vladimir.hutanu@frm2.tum.de).

Color versions of one or more figures in this article are available at https://doi.org/10.1109/TMAG.2021.3082983.

Digital Object Identifier 10.1109/TMAG.2021.3082983

TABLE I
CRYSTAL DATA OF $Ba_2CoGe_2O_7$

Space group		$P\bar{4}2_1m$		
a [Å]		8.346(3)		
c [Å]		5.500(19)		
Ion	Wyckoff position	x	y	z
Ba	$4e$	0.33465(14)	0.16537(14)	0.49239(28)
Co	$2b$	0	0	0
Ge	$4e$	0.14085(11)	0.35915(11)	0.04031(19)
O1	$2c$	0	0.5	0.15996(39)
O2	$4e$	0.13802(16)	0.36200(16)	0.72960(27)
O3	$8f$	0.07906(15)	0.18452(14)	0.18825(20)

Details about the crystal structure and the atom positions for $Ba_2CoGe_2O_7$ at 10.4 K taken from Ref. [9].

Polarized neutron diffraction (PND) was recently introduced as one of the most suitable methods to determine the absolute DMI-sign in WFM materials [11]. PND provides a direct access to the scattering contribution from nuclear-magnetic interference and thus reveals the phase difference between the nuclear and magnetic structures. This permits to determine the absolute direction of the individual magnetic moments with respect to the atomic arrangement, distinguishing between two equivalent AFM arrangements that correspond to either a positive or negative DMI sign.

Here, we report on a detailed PND study of the ordered magnetic moment in $Ba_2CoGe_2O_7$ to determine for the first time the sign of the DMI in this interesting compound. This will give a valuable insight in its fundamental exchange interactions and provide a set of high-quality reference data for testing and validating different theoretical or numerical models for its unconventional multiferroicity in the future studies. The findings are supported by a detailed symmetry analysis of the DMI vector in $Ba_2CoGe_2O_7$, straightforwardly applicable to further structures and compounds.

II. SYMMETRY ANALYSIS

$Ba_2CoGe_2O_7$ crystallizes in the melilite-typical space group $P\bar{4}2_1m$ (No. 113 International Tables) [9]. The crystal structure parameters at low temperature are shown in Table I and the atomic arrangement is shown in Fig. 1. The non-magnetic atoms of Ge, Ba, and O situated at the $4e$ and $8f$ Wyckoff positions lift the inversion centers between the magnetic Co atoms at the $2b$ positions and, thus, provide the basic requirement for the emergence of the DMI, according to the first rule determined by Moriya [3]. In general, the DMI energy of two atoms at positions $\boldsymbol{r}_1$ and $\boldsymbol{r}_2$ with magnetic moments $\boldsymbol{m}_1$ and $\boldsymbol{m}_2$ is given by $\boldsymbol{D}_{12} \cdot (\boldsymbol{m}_1 \times \boldsymbol{m}_2)$ with $\boldsymbol{D}_{12}$ the antisymmetric DMI vector parameter (i.e., $\boldsymbol{D}_{12} = -\boldsymbol{D}_{21}$). Since the DMI energy has to be invariant upon all symmetry operation of O(3), D_{12} must be an axial vector similar to $\boldsymbol{m}_1 \times \boldsymbol{m}_2$. This means that the DMI vector on a $\boldsymbol{r}_{\mathcal{S}1}$–$\boldsymbol{r}_{\mathcal{S}2}$ bond is related to the DMI vector on a $\boldsymbol{r}_1$–$\boldsymbol{r}_2$ bond according to

$$\boldsymbol{D}_{\mathcal{S}1\mathcal{S}2} = \det[\mathcal{R}]\,\mathcal{R}[\boldsymbol{D}_{12}] \tag{1}$$

if the two bonds are connected by a space group symmetry operation $\mathcal{S}$, where $\mathcal{R}$ is the point group part of $\mathcal{S}$. Utilizing the antisymmetric properties of $\boldsymbol{D}$ with 1 results in the symmetry restriction $\boldsymbol{D}_{12} = \mp\det[\mathcal{R}]\,\mathcal{R}[\boldsymbol{D}_{12}]$ for the DMI vector if operation $\mathcal{S}$ interchanges $\boldsymbol{r}_1$ and $\boldsymbol{r}_2$ $(-)$ or leaves them unchanged $(+)$. This basic restriction reproduces well the general rules for the DMI vector determined by Moriya [3], as shown in [11].

To determine the symmetry restrictions on the DMI vector in $Ba_2CoGe_2O_7$ imposed by space group $P\bar{4}2_1m$, we focus on the magnetic cobalt atoms at $\boldsymbol{r}_1 = (0, 0, 0)$ and $\boldsymbol{r}_2 = ((1/2), (1/2), 0)$. These two sites are interchanged by symmetry operation $(1/2) - y, (1/2) - x, z$ (mirror plane normal to [110], followed by a translation for $(1/2)$ along [110]). Applying 1 to this symmetry operation restricts the in-plane components of the DMI vector to $D_{12x} = -D_{12y}$ and, thus, $\boldsymbol{D}_{12}$ to the plane perpendicular to the connection vector $\boldsymbol{d}_{12} = \boldsymbol{r}_2 - \boldsymbol{r}_1$. To determine the DMI relation of neighboring bonds, we consider additionally the cobalt atom at $\boldsymbol{r}_{1'} = (1, 0, 0)$, a symmetry equivalent position to $\boldsymbol{r}_1$. The symmetry operation $(1/2) + x, (1/2) - y, -z$ (twofold rotation around the x-axis, followed by a translation for $(1/2)$ along [110]) maps $\boldsymbol{r}_1$ to $\boldsymbol{r}_2$ and $\boldsymbol{r}_2$ to $\boldsymbol{r}_{1'}$. Thus, application of 1 defines the DMI vector as $\boldsymbol{D}_{1'2} = \left(-D_{12x}, -D_{12x}, D_{12z}\right)$, which is again perpendicular to the respective connection vector $\boldsymbol{d}_{1'2}$. Analogously, the connection between the DMI vectors of all remaining cobalt pairs in the unit cell can be deduced, resulting in a DMI vector pattern as shown in Fig. 1, characterized by an alternating in-plane and a uniform out-of-plane component.

Below $T_N = 6.7$ K, $Ba_2CoGe_2O_7$ orders antiferromagnetically in the ab plane with sublattices A and B belonging to the cobalt atoms at $\boldsymbol{r}_1$ and $\boldsymbol{r}_2$, respectively [9], [12]. By averaging the DMI energy of a cobalt atom with its four nearest neighbors of the other sublattice, the in-plane component cancels out and only the uniform D_{12z} component remains, as clearly visible in Fig. 1. This D_{12z} component, which will be denoted as D_z in the following, induces a small canting in the otherwise collinear AFM structure, leading to an in-plane WFM moment of around $0.009\,\mu_B$/Co [1]. If this WFM moment is aligned by an external magnetic field applied in the ab plane, the sign of the D_z component determines which of the two possible AFM arrangements is energetically favored, i.e., minimizes $D_{12z}(\boldsymbol{m}_A \times \boldsymbol{m}_B)_z$. For an applied magnetic field along the [100] direction, this is shown in Fig. 1(a) and (b) for a negative and positive D_z components, respectively.

In general, we can split the magnetic moment of each sublattice into a ferromagnetic (FM) part $\boldsymbol{m}_A^{\mathrm{FM}} = \boldsymbol{m}_B^{\mathrm{FM}} = (\boldsymbol{m}_A + \boldsymbol{m}_B)/2$, pointing for both sublattices in the same direction, and an AFM part $\boldsymbol{m}_A^{\mathrm{AFM}} = -\boldsymbol{m}_B^{\mathrm{AFM}} = (\boldsymbol{m}_A - \boldsymbol{m}_B)/2$, which reverses its sign between the sublattices (see detailed view in the dotted circles in Fig. 1). Due to the higher symmetry of the magnetic lattice compared to the symmetry of the complete unit cell and the 2-D AFM structure in the tetragonal plane, $\boldsymbol{m}_A^{\mathrm{FM}}$ contributes only to (hkl) Bragg reflections with even $h + k$ indices (so-called FM-type reflections), whereas $\boldsymbol{m}_A^{\mathrm{AFM}}$ contributes only to the reflections with odd $h + k$ indices

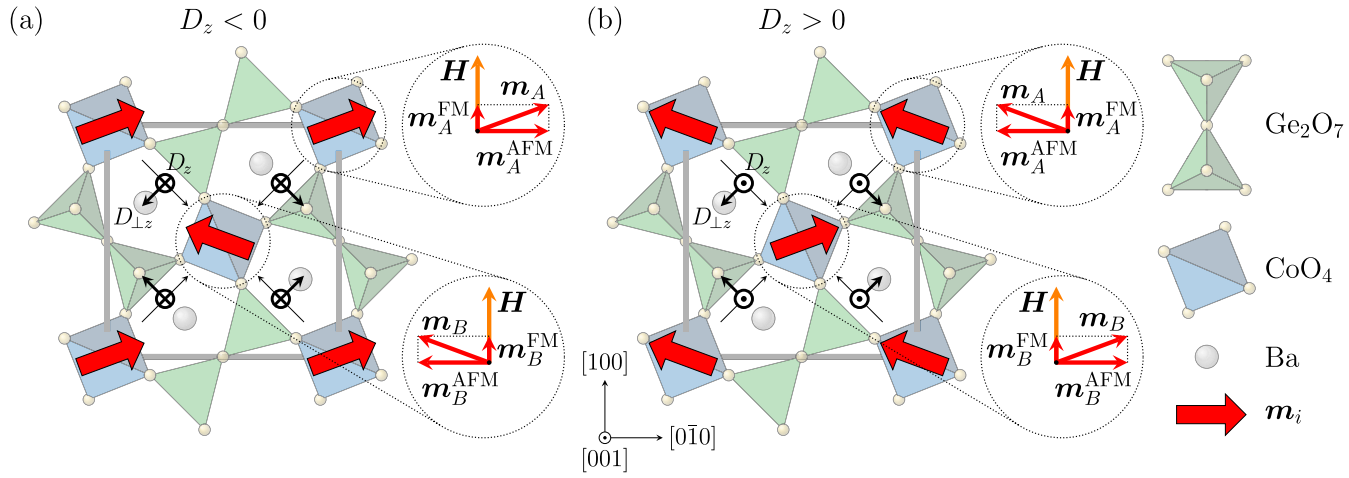

Fig. 1. Atomic arrangement in the unit cell of $Ba_2CoGe_2O_7$ as defined in [7] (Table II). The germanium and cobalt atoms are located in the center of the blue and green tetrahedrons, respectively. The oxygen atoms are shown as yellow spheres. The barium atoms, which are located between two CoO_4/Ge_2O_7 layers, are shown as gray spheres. The thick black arrows between the magnetic CoO_4 groups indicate the arrangement of the in-plane ($D_{\perp z}$) and out-of-plane (D_z) DMI vector component for bonding directions as given by the thin black arrows. If the bonding direction is reversed, the DMI vector components will switch sign. Panels (a) and (b) show the two possible magnetic moment configurations stabilized depending on the sign of D_z by applying an external magnetic field $\boldsymbol{H}$ along the [100] direction and thus, aligning the WFM moment along $\boldsymbol{H}$. (a) $D_z < 0$. (b) $D_z > 0$.

(AFM-type reflections). Thus, each part of the magnetization can be independently investigated by diffraction. Note that the AFM- and FM-type reflections are split by the parity of $h+k$ in $Ba_2CoGe_2O_7$ unlike as in the previously studied $MnCO_3$ and α-Fe_2O_3 in [11] where they are split by the parity of l since the AFM sublattice mixing in these compounds is along the c direction and not in the tetragonal plane.

III. Experimental Setup and Sample

High-quality single crystal of $Ba_2CoGe_2O_7$ was grown by the floating zone method. The sample has a cylindrical shape of about 6 mm in diameter and similar length and is well characterized by previous studies [8]. PND measurements were performed at the polarized diffractometer VIP at the Orphée reactor of LLB (Saclay, France) [13]. The pre-oriented crystal was placed in a vertical high magnetic field of up to 6 T and the asymmetry values $A = (I^+ - I^-)/(I^+ + I^-)$ of all available Bragg reflections were measured. Here, $I^{\pm}$ denotes the measured intensity for the two antiparallel spin orientations of the incoming neutron beam in regard to the quantization axis of the field. Due to the short neutron wavelength of 0.84 Å and the large 2-D detector at VIP, a good q-coverage could be achieved (a large number of observations).

IV. Experimental Results

With the a-axis of the crystal mounted vertical and, thus, parallel to the applied magnetic field of 6 T, the asymmetry values of overall 611 Bragg reflections, among them 290 of FM-type and 321 of AFM-type, were collected at a temperature of 2 K in the WFM phase. In this configuration, the FM part of the magnetization, consistent of the field-aligned WFM and field-induced FM moment, is expected to be parallel to the field direction, whereas the AFM part should be directed in the ab plane perpendicular to $\boldsymbol{H}$. Although the crystal [100] direction was pre-aligned to the vertical instrument axis, a slight tilt of $-3.2(2)^\circ$ in the ab plane toward the b-axis (see Fig. 2) and $9.4(4)^\circ$ toward the c-axis was observed by refining the experimental orientation matrix. To take this into account, an orthogonal set of axes is defined with x parallel to $\boldsymbol{H}$ and y in the ab plane perpendicular to $\boldsymbol{H}$ and thus parallel to $c \times \boldsymbol{H}$. The z-axis forms the right-handed completion of x and y and is approximately parallel to the crystal [001] direction. This orthogonal system is shown in Fig. 2.

To precisely determine the ordered magnetic moment values in $Ba_2CoGe_2O_7$, the collected set of asymmetry values was refined with the MAG2POL program [14] using the crystal structure as previously reported by Hutanu *et al.* [7]. For the refinement, extinction was considered. Further parasitic effects such as absorption, which only scale the absolute intensity of the individual Bragg reflections, can be neglected due to the refinement on asymmetries rather than intensities. Without applying any restrictions on the moment directions, a total sublattice magnetization of 2.57(9) μ_B is obtained, which is in good agreement with previous non-polarized neutron studies [9]. The results of the refinement for the individual components of the magnetic moment are shown in Table II and denoted as "restriction-free." For the FM part ($\boldsymbol{m}_A^{\mathrm{FM}}$), a significant contribution is only obtained along x, the magnetic field direction. This value can be used to determine an in-plane susceptibility of 0.152(3) (μ_B/T)/Co, reproducing well macroscopic studies [1], [4]. In contrast, the AFM part ($\boldsymbol{m}_A^{\mathrm{AFM}}$) is found to be almost parallel to y, the direction perpendicular to $\boldsymbol{H}$ in the ab plane. These results agree well with our expectations discussed previously; therefore, it is reasonable to restrict $\boldsymbol{m}_A^{\mathrm{FM}}$ parallel to the field direction and $\boldsymbol{m}_A^{\mathrm{AFM}}$ perpendicular to it. The detailed results of this restricted refinement are also given in Table II and show no significant change of both refined moments and fit quality.

The refined magnetic moment arrangement is visualized in the left panel of Fig. 2. By comparison with the two possible spin configurations for a negative and positive sign

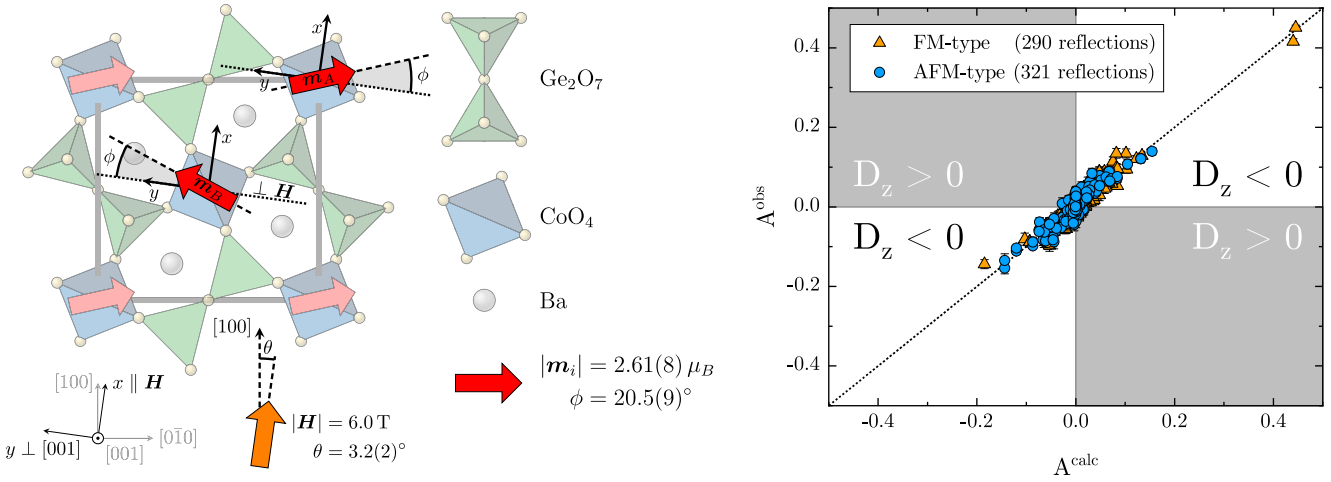

Fig. 2. Results of the symmetry restricted magnetic moment refinement in $Ba_2CoGe_2O_7$ from Table II. The left-hand side shows the projection of the exact field direction (orange arrow) and the resulting magnetic moment configuration (red arrows) on the *ab* plane. The in-plane tilt angle of the magnetic field is drawn exaggerated to be visible. In addition, the orthogonal x, y, and z directions used in the text are defined. The right-hand side shows the comparison between the observed and calculated asymmetry values for the refinement, separately for FM-type ($h + k$ even) and AFM-type ($h + k$ odd) reflections.

TABLE II
RESULTS OF THE MAGNETIC MOMENT REFINEMENT

Component	Restriction	m_x (μ_B)	m_y (μ_B)	m_z (μ_B)	χ_r^2
$\boldsymbol{m}_A^{\mathrm{FM}}$	free	0.91(2)	0.03(9)	0.07(8)	1.88
$\boldsymbol{m}_A^{\mathrm{AFM}}$	free	0.03(2)	−2.40(9)	−0.15(8)	1.63
$\boldsymbol{m}_A^{\mathrm{FM}}$	$\parallel \boldsymbol{H}$	0.91(2)	0	0	1.88
$\boldsymbol{m}_A^{\mathrm{AFM}}$	$\perp \boldsymbol{H}$	0	−2.44(9)	−0.09(7)	1.64

Overview of the results of the refinement using free or symmetry restricted magnetic moments for the collected data set of 611 asymmetries in $Ba_2CoGe_2O_7$ at 2 K. The components of the magnetization vector refer to the xyz directions defined in Fig. 2.

of D_z determined by symmetry analysis in Section II and shown in Fig. 1(a) and (b), respectively, a negative sign of the DMI in $Ba_2CoGe_2O_7$ can be unambiguously determined here for the first time. The good quality of the refinement (reduced chi squared values χ_r^2 given in Table II for FM- and AFM-type reflections separately) is shown in the right panel of Fig. 2 as a comparison between the calculated and observed asymmetry values. It is important to note that the sign of the asymmetry for an AFM-type reflection is directly related to the sign of $\boldsymbol{m}_A^{\mathrm{AFM}}$ and thus is inverted between the two spin configurations shown in Fig. 1(a) and (b). As we used the spin configuration shown in Fig. 1(a) for the calculation of A^{calc}, the sign of all the asymmetry values of AFM-type reflections within the two white areas is correctly reproduced by the $D_z < 0$ spin configuration and thus confirm the negative sign of the determined D_z component. If we had instead used the spin configuration shown in Fig. 1(b) for the calculation of A^{calc}, its sign would reverse for all AFM-type reflections and asymmetry values in the two gray areas of Fig. 2 would have been obtained, showing that the spin configuration of Fig. 1(b) is not the correct one. Likewise, if the actual spin configuration was the one shown in Fig. 1(b) and we used the model shown in Fig. 1(a), asymmetries would have also been in the gray areas, invalidating for the calculation assumed spin configuration and suggesting a positive D_z sign. In fact,

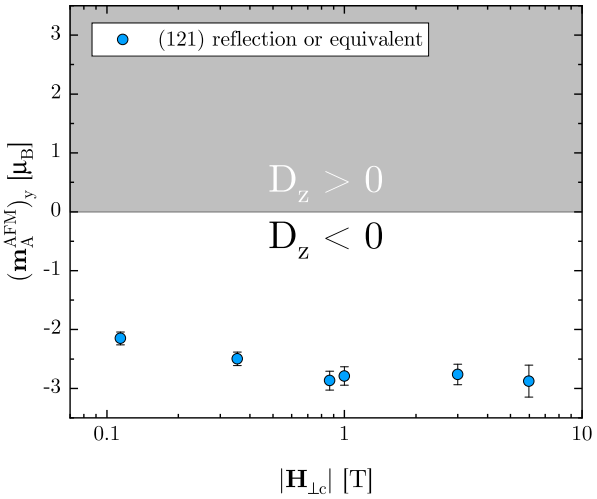

Fig. 3. AFM moment of sublayer A directly calculated from the asymmetry values of the (121) reflection or equivalent for different magnetic field values and directions. For the calculation, the AFM moment was assumed to be in *ab* plane perpendicular to the magnetic field, corresponding to the y direction defined in Fig. 2. Temperature factor and extinction correction were neglected. The calculated magnetic moment values are shown dependent on the value of the in-plane component of the applied magnetic field, which saturates the single domain state.

the measurement of a single strong AFM-type reflection is sufficient to unambiguously determine the DMI sign by PND.

To emphasize this unique strength of PND, especially useful for compounds with a small accessible q-range or low counting rates, which prevents large data collections for a complete refinement, we have selected the single strong AFM-type (121) reflection for a focused study. In this scope, we collected the asymmetries for the (121) reflection or its symmetry equivalent for different directions and values of the applied magnetic field. Using the common equations for the nuclear and magnetic scattering factor [15] and the spherical approximation of the magnetic form factor of Co^{2+} provided by Brown [16], one can calculate the expected

y component of $\boldsymbol{m}_A^{\mathrm{AFM}}$ directly from the measured asymmetry value. As defined previously [Fig. 2 (left)], the y-axis is parallel to $c \times \boldsymbol{H}$. For the calculation, the temperature factors and extinction correction were dismissed, as they may only slightly influence the determined magnetic moment value, but not its sign. Fig. 3 shows the resulting y component of the AFM moment in dependence of the in-plane applied magnetic field. A slight saturation behavior, most probably related to the WFM domains, could be observed at low field values. As $\boldsymbol{m}_A^{\mathrm{FM}}$ is aligned by the magnetic field and, thus, points in the positive x direction, the average DMI energy is given by $-2D_z(\boldsymbol{m}_A^{\mathrm{AFM}})_y(\boldsymbol{m}_A^{\mathrm{FM}})_x \cos\rho$, with ρ the out-of-plane angle of the applied magnetic field. Therefore, D_z and the y component of $\boldsymbol{m}_A^{\mathrm{AFM}}$ must be same-signed to be energetically favorable. Since Fig. 3 shows clearly a negative AFM moment over the complete field range covering almost two orders of magnitude, we can conclude from the experimentally determined asymmetry of a single reflection about the negative DMI sign in $Ba_2CoGe_2O_7$ in the whole studied field region. This is in agreement with the results from the refinement and demonstrates the high reliability of the presented PND method and its universality in regard to the applied field direction and value.

V. Conclusion

Using a detailed symmetry analysis and PND within this study, we determined for the first time the absolute sign of the DMI in the peculiar non-centrosymmetric multiferroic $Ba_2CoGe_2O_7$. By refining the PND data, the precise spin arrangement under an applied magnetic field could be established. The refined value for the overall ordered magnetic moment of $2.61(8)\,\mu_B$/Co is in good agreement with previous polarized and non-polarized neutron diffraction studies. Both field-induced FM and field-orthogonal AFM components could be precisely separated and their evolution with applied magnetic fields in the range between 0.1 and 6 T studied. An in-plane susceptibility of $0.152(3)\,(\mu_B/\mathrm{T})$/Co was experimentally determined and agrees well with previous macroscopic studies. It is demonstrated that the applied method (PND) provides reliable results on the DMI-sign determination, even using only a single suitable Bragg reflection. This opens the perspectives of its application to the large class of WFM materials.

Acknowledgment

The work was supported under the Tasso Springer Fellowship Program and the Jülich-Aachen Research Alliance (JARA).

References

[1] H. T. Yi, Y. J. Choi, S. Lee, and S.-W. Cheong, "Multiferroicity in the square-lattice antiferromagnet of $Ba_2CoGe_2O_7$," *Appl. Phys. Lett.*, vol. 92, no. 21, May 2008, Art. no. 212904.

[2] I. E. Dzyaloshinskii, "Thermodynamical theory of 'weak' ferromagnetism in antiferromagnetic substances," *Sov. Phys., JETP*, vol. 5, no. 6, pp. 1259–1272, 1957.

[3] T. Moriya, "Anisotropic superexchange interaction and weak ferromagnetism," *Phys. Rev.*, vol. 120, no. 1, pp. 91–98, Oct. 1960.

[4] H. Murakawa, Y. Onose, S. Miyahara, N. Furukawa, and Y. Tokura, "Ferroelectricity induced by spin-dependent metal-ligand hybridization in $Ba_2CoGe_2O_7$," *Phys. Rev. Lett.*, vol. 105, no. 13, Sep. 2010, Art. no. 137202.

[5] P. Toledano, D. D. Khalyavin, and L. C. Chapon, "Spontaneous toroidal moment and field-induced magnetotoroidic effects in $Ba_2CoGe_2O_7$," *Phys. Rev. B, Condens. Matter*, vol. 84, no. 9, Sep. 2011, Art. no. 094421.

[6] M. Soda *et al.*, "Spin-nematic interaction in the multiferroic compound $Ba_2CoGe_2O_7$," *Phys. Rev. Lett.*, vol. 112, no. 12, Mar. 2014, Art. no. 127205.

[7] V. Hutanu, A. Sazonov, H. Murakawa, Y. Tokura, B. Náfrádi, and D. Chernyshov, "Symmetry and structure of multiferroic $Ba_2CoGe_2O_7$," *Phys. Rev. B, Condens. Matter*, vol. 84, no. 21, Dec. 2011, Art. no. 212101.

[8] A. Sazonov *et al.*, "Origin of forbidden reflections in multiferroic $Ba_2CoGe_2O_7$ by neutron diffraction: Symmetry lowering or Renninger effect?" *J. Appl. Crystallogr.*, vol. 49, no. 2, pp. 556–560, Apr. 2016.

[9] V. Hutanu *et al.*, "Determination of the magnetic order and the crystal symmetry in the multiferroic ground state of $Ba_2CoGe_2O_7$," *Phys. Rev. B, Condens. Matter*, vol. 86, no. 10, Sep. 2012, Art. no. 104401.

[10] J. M. Perez-Mato and J. L. Ribeiro, "On the symmetry and the signature of atomic mechanisms in multiferroics: The example of $Ba_2CoGe_2O_7$," *Acta Crystallographica Sect. A Found. Crystallogr.*, vol. 67, no. 3, pp. 264–268, May 2011.

[11] H. Thoma *et al.*, "Revealing the absolute direction of the Dzyaloshinskii–Moriya interaction in prototypical weak ferromagnets by polarized neutrons," *Phys. Rev. X*, vol. 11, no. 1, Mar. 2021, Art. no. 011060.

[12] T. Sato, "Magnetic property of $Ba_2CoGe_2O_7$," *Phys. Rev. B, Condens. Matter*, vols. 329–333, no. II, pp. 880–881, May 2003.

[13] A. Gukasov *et al.*, "Very intense polarized (VIP) neutron diffractometer at the ORPHEE reactor in saclay," *Phys. Procedia*, vol. 42, pp. 150–153, 2013.

[14] N. Qureshi, "Mag2Pol: A program for the analysis of spherical neutron polarimetry, flipping ratio and integrated intensity data," *J. Appl. Crystallogr.*, vol. 52, no. 1, pp. 175–185, Feb. 2019.

[15] G. L. Squires, *Introduction to the Theory of Thermal Neutron Scattering*, 3rd ed. Cambridge, U.K.: Cambridge Univ. Press, May 2012.

[16] P. J. Brown, *Magnetic Form Factors*. Dordrecht, The Netherlands: Springer, 2006, ch. 4, pp. 454–461.